Journal of the European Ceramic Society 23 (2003) 773–780

www.elsevier.com/locate/jeurceramsoc

# Mechanical properties and microstructure for 3 mol% yttria doped zirconia/silicon carbide nanocomposites

Noriko Bamba[a,*], Yong-Ho Choa[b], Tohru Sekino[c], Koichi Niihara[c]

[a]*Department of Electric and Electronic Engineering, Facuty of Engineering, Shinshu University, 4-17-1 Wakasato, Nagano 380-8553, Japan*
[b]*Department of New Materials Technology, Hanyang University, 1271 Sa-1, Ansan, Kyungki Do 425-791, Republic of Korea*
[c]*The Institute of Scientific and Industrial Research, Osaka University, 8-1 Mihogaoka, Ibaraki, Osaka 567-0047, Japan*

Received 8 December 2001; received in revised form 2 May 2002; accepted 12 May 2002

**Abstract**

3 Mol% yttria stabilized tetragonal zirconia polycrystalline (3Y-TZP) is well known as a transformation toughening material with excellent mechanical properties at ambient temperature. However, the properties of 3Y-TZP drop down with increasing temperature. In this study, nanocomposite techniques were applied in order to improve mechanical properties of 3Y-TZP. 3Y-TZP/SiC nanocomposites were fabricated by hot-pressing, and effects of SiC particles on microstructure, transformation from tetragonal zirconia (t-$ZrO_2$) to monoclinic $ZrO_2$ (m-$ZrO_2$) and its mechanical properties were investigated. Fracture toughness of the nanocomposite was improved without decrease of strength. This should be due to not only crack deflection by dispersed SiC particles with high Young's modulus, but also the phase transformation of t-$ZrO_2$ accelerated by the residual stresses from coefficient of thermal expansion mismatch between 3Y-TZP and SiC.


*Keywords:* Mechanical properties; Nanocomposites; SiC inclusions; Toughness; $ZrO_2$

## 1. Introduction

Zirconia ($ZrO_2$) can possess various strength/toughness ratios by varying a kind of stabilizer, e.g. $Y_2O_3$, CeO and MgO, and content of stabilizer,[1–3] and the properties also depend on microstructure of sintered bodies.[4,5] Yttria stabilized tetragonal $ZrO_2$ (Y-TZP) exhibits excellent mechanical properties; the maximum strength is over 1.5 GPa for 2.5 mol% Y-TZP and the maximum toughness about 15 MPa $m^{1/2}$ for 2 mol% Y-TZP.[1] Swain et al.[6,7] suggested a mechanism for the limitation of strength in transformation toughened $ZrO_2$ system, and it is difficult to improve both strength and toughness only by transformation toughening. These excellent properties are due to the stress-induced transformation from tetragonal (t-$ZrO_2$) to monoclinic (m-$ZrO_2$) phase, which are obtained only at ambient temperature. The properties dramatically decrease with increasing temperature, because the t-$ZrO_2$ to m-$ZrO_2$ transformation toughening effect decreases at higher temperatures with increasing of t-$ZrO_2$ phase stability. Additionally, annealing at low temperatures, about 200 °C, also degrades the mechanical properties.[8,9]

Various methods have been applied to improve the properties, and composite technique that secondary reinforcing phases such as whiskers, platelets, fibers or particles are dispersed in matrix, is one of most effective methods and widely used.[10–15] Recent researches have reported that ceramic composites incorporating nano-size particulate within matrix grains or at the grain boundaries (denoted by nanocomposites) possess excellent mechanical properties, even at high temperatures.[16–23] This is due to crack deflection and inhibition of grain boundary sliding at elevated temperatures by dispersed phase and residual stresses based on mismatch of coefficients of thermal expansion (CTE) between matrix material and dispersoid. Therefore the nanocomposite techniques were applied for 3 mol% $Y_2O_3$ doped $ZrO_2$ (3Y-TZP), and 3Y-TZP/SiC nanocomposites were fabricated to improve both strength and toughness. SiC particulate was used as a second phase in this study, because it has much lower CTE than 3Y-TZP, high Young's modulus and excellent

* Corresponding author.
*E-mail address:* nbamba@gipwc.shinshu-u.ac.jp (N. Bamba).

0955-2219/02/$ - see front matter © 2002 Published by Elsevier Science Ltd.
PII: S0955-2219(02)00168-1

mechanical properties at elevated temperatures. Additionally, improvements in thermal conductivity and thermal stability, such as degradation of mechanical properties by low and high temperatures annealing, are also expected.

The objects of the present work are to evaluate the mechanical properties of 3Y-TZP/SiC nanocomposite fabricated by hot-pressing and investigate effects of SiC particulate on microstructure, t-$ZrO_2$ to m-$ZrO_2$ transformation and its mechanical properties. The relationships between transformation toughening and grain size and/or the residual stresses were discussed.

## 2. Experimental procedure

3Y-TZP powder with average crystalline size of 20 nm (Sumitomo Osaka Cement Co., Ltd.) and β-SiC powder with average grain size of 150 nm (Mitsui touatsu kagaku Ltd.) were used as a matrix and a second phase, respectively. 3Y-TZP and β-SiC which was 0, 5 and 20 vol.% to 3Y-TZP content were ball-milled in $C_2H_5OH$ for 48 h with $ZrO_2$ ball. After dry, the mixed powders were dry ball-milled for 12 h, which were sieved under 150 μm to remove hard agglomerate particles. The powders were hot-pressed at 1350–1850 °C for 1 h under 30 MPa in Ar atmosphere by using carbon heater. The sintered bodies were cut and ground into rectangular bar specimens ($4\times3\times36$ $mm^3$), and polished using diamond paste with 0.5 μm to evaluate microstructure and mechanical properties.

Density of specimens was determined by the Archimedes method using toluene, and Young's modulus was evaluated by the resonance method. Fracture strength was measured by the three-point bending test (span: 30 mm, crosshead speed: 0.5 mm/min). Fracture toughness was evaluated for the specimens before and after annealing from the indentation fracture (IF) test[24] with 196 N load at room temperature. Annealing was carried out at 1300 °C for 10 min in Ar, in order to eliminate transformed phase (m-$ZrO_2$) which was generated by machining. X-ray diffraction (XRD) analyses were performed on both polished and fracture surfaces to identified the phases in each specimen and assess m-$ZrO_2$ content. The volume fraction of the m-$ZrO_2$, $V_m$, was calculated by using the following equations,[25]

$$V_m = PX_m/(1 + (P-1)X_m) \quad (1)$$

where $X_m$ is the integrated intensity ratio expressed by Eq. (2) and $P = 1.311$

$$X_m = \left(I_m(111) + I_m(\bar{1}11)\right)/\left(I_m(111) + I_m(\bar{1}11) + I_t(111)\right) \quad (2)$$

$I$ is the integrated intensity, and subscripts m and t indicate the m-$ZrO_2$ and the t-$ZrO_2$, respectively. The microstructure studies were performed through scanning electron microscopy (SEM) and transmission electron microscopy (TEM). The samples for SEM observation were thermally etched at 1300–1450 °C for 10 min in Air for 3Y-TZP monolith and in Ar for the composites, respectively. The specimens for TEM observation were ground down to about 150 μm, which were ion beam thinning after dimpling. Grain size and its distribution were analyzed from SEM photographs by using an image analysis technique (NIH image written by Wayne Rasband at U.S. National Institutes of Health and available from the Internet by anonymous ftp from zippy.nimh.nih.gov or on floppy disk from NTIS, 5285 Port Royal Rd., Springfield, VA 22161, part number PB93–504868).

## 3. Results

3Y-TZP monolith, 3Y-TZP/5 and 20 vol% SiC nanocomposites (denoted by 3Y5S and 3Y20S) were fabricated. XRD analysis showed that all composites consisted of mainly t-$ZrO_2$, a little m-$ZrO_2$ and β-SiC, no reaction phase was detected. This result was different from the result by Ding et al.[26] Reductive atmosphere produced by carbon heater may suppress reactions between $ZrO_2$ and SiC. High-resolution transmission electron microscopic (HRTEM) image as shown in Fig. 1 also exhibited that no reaction phase existed at the interface between 3Y-TZP matrix grain and SiC particle. Glassy phase due to impurities in raw powders, however, was observed at some of triple points. Fig. 2 shows a TEM image of the 3Y5S sintered at 1700 °C (3Y5S1700), which indicates that SiC particulate was homogeneously dispersed within 3Y-TZP matrix grains and/or at grain boundaries. SiC particles with submicro meter in particle size were mainly located at grain boundaries, while finer ones were within matrix grains.

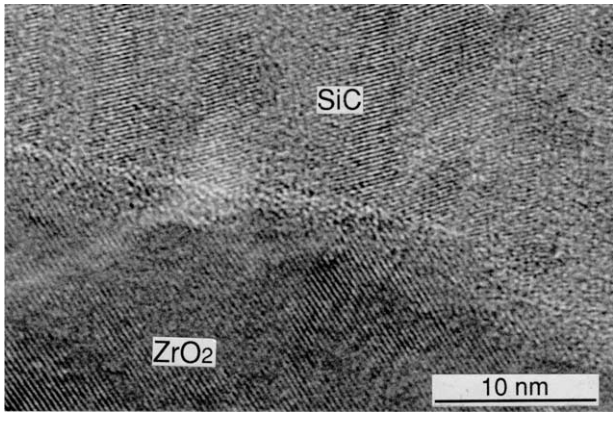


Fig. 1. High resolution transmission electron microscopy image of 3Y-TZP/5 vol.% SiC nanocomposite sintered at 1700 °C.

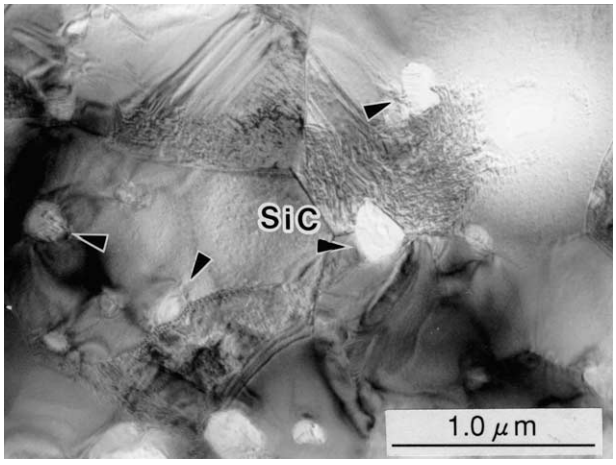


Fig. 2. TEM image of 3Y-TZP/5 vol.% SiC nanocomposite sintered at 1700 °C.

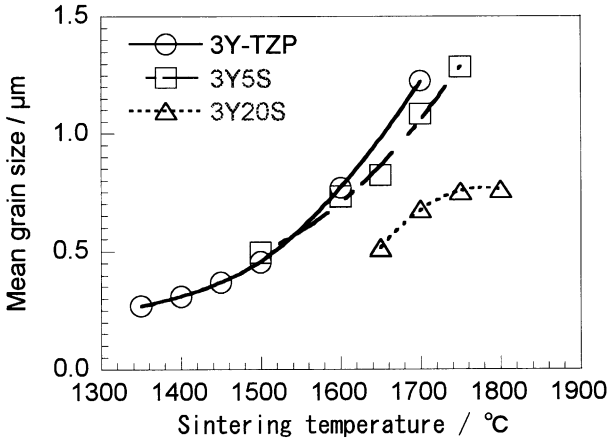


Fig. 4. The mean grain size as a function of sintering temperature for 3Y-TZP monolith and 3Y-TZP/SiC nanocomposites.

Larger SiC particles suppress grain boundary movement of matrix. For this reason, larger particles remained at grain boundary. Dislocation can be observed around intragranular SiC particle due to relaxation of the stress caused by CTE mismatch. The mismatch generates high residual tensile and/or compressive stresses in nanocomposite materials. In the case of 3Y5S1700, about 60 MPa tensile stress might be imposed on matrix and 1200 MPa compressive stress on SiC particles.[27]

Fig. 3 indicates the variation of relative density with sintering temperature. The densification was suppressed by SiC addition, however, fully densified body could be obtained in each composition. For monolith, fully dense sample was obtained at 1450 °C, while 1500 and 1750 °C were required for 3Y5S and 3Y20S, respectively. The sintering temperatures for fully densified bodies became higher with increasing SiC content.

Fig. 4 shows the mean matrix grain size as a function of sintering temperature. Grain growth of 3Y-TZP matrix was suppressed by fine SiC particles as well as densification, and grain growth became smaller with increase in amount of SiC content. The grain size distributions for 3Y-TZP monolith, 3Y5S and 3Y20S sintered at 1700 °C (3Y-TZP1700, 3Y5S1700 and 3Y20S1700) are shown in Fig. 5. Compared with the monolith, nanocomposites had a narrow grain size distribution, especially 3Y20S. The 3Y-TZP1700 had exaggerated grains with about 4.1 μm in grain size, while the maximum grain size of the 3Y5S1700 and 3Y20S1700 were 2.5 and 1.9 μm, respectively. Nanosized SiC dispersoid inhibited not only normal grain growth but also abnormal grain growth. Nanocomposite systems had fine and homogeneous microstructure.

Fig. 6 shows the variation of Young's modulus with sintering. Young's moduli for all composition increased with the density as described in Fig. 3, and with volume fraction of SiC. These constant values after densified coincided with theoretical values calculated by using the rule of mixture for spherical dispersoids.[28]

The variations of fracture strength with sintering temperature are shown in Fig. 7. The strength rose with increasing density, and then, the maximum strength in each composition was over 1.5 GPa. There were little

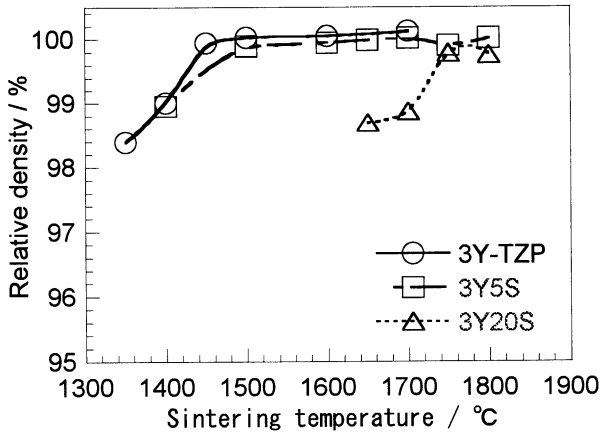


Fig. 3. The variation of relative density with sintering temperature for 3Y-TZP monolith and 3Y-TZP/SiC nanocomposites.

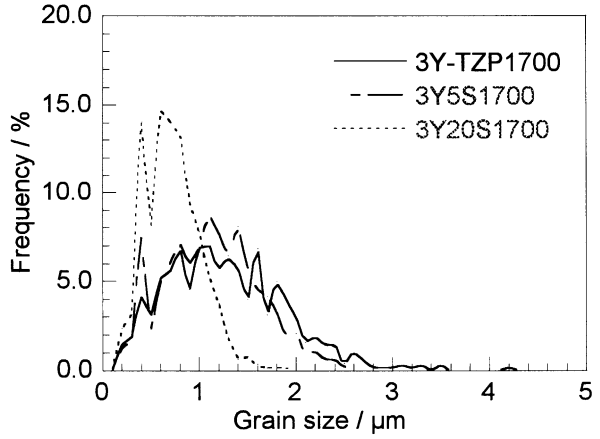


Fig. 5. The grain size distribution of for 3Y-TZP monolith and 3Y-TZP/SiC nanocomposites sintered at 1700 °C.

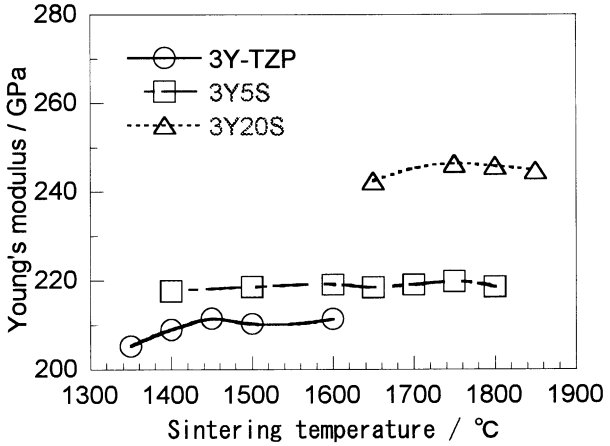


Fig. 6. The variation of Young's modulus for 3Y-TZP monolith and 3Y-TZP/SiC nanocomposites with sintering temperature. Young's modulus increased as SiC content increased.

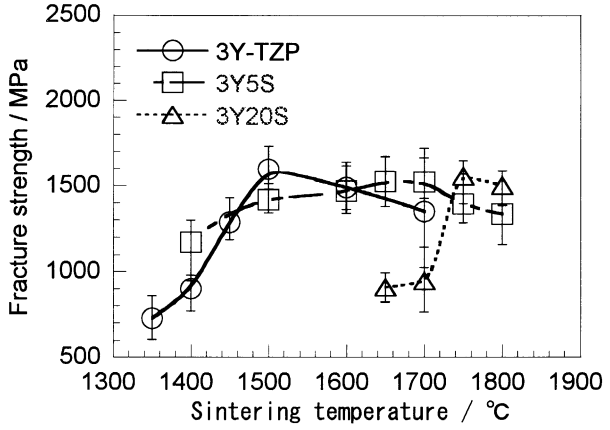


Fig. 7. The fracture strength for 3Y-TZP monolith and 3Y-TZP/SiC nanocomposites as a function of sintering temperature.

differences between the monolith and composites. No effect of SiC particles on strength was observed.

Fracture toughness as a function of sintering temperature for 3Y-TZP monolith, 3Y5S and 3Y20S before and after annealing at 1300 °C for 10 min in Ar flow are shown in Fig. 8. Annealing changed m-$ZrO_2$ on the polished surface to t-$ZrO_2$. The nanocomposites exhibited superior toughness to the monolith both before and after annealing. The toughness of both the monolith and composites decreased by annealing, which is due to the elimination of the surface imposed by residual compressive stress through machining. The stress gives an improvement in the toughness.[29] It was confirmed by XRD analysis that m-$ZrO_2$ existed on the polished surface before annealing, however, the m-$ZrO_2$ conversely transformed to t-$ZrO_2$ after annealing. With increasing sintering temperature, the toughness for the monolith and the composites were improved, because transformation from t-$ZrO_2$ to m-$ZrO_2$ can occur easily with increasing in grain size.[4] Fig. 9 indicates m-$ZrO_2$ content in fracture surface as a function of sintering temperature.

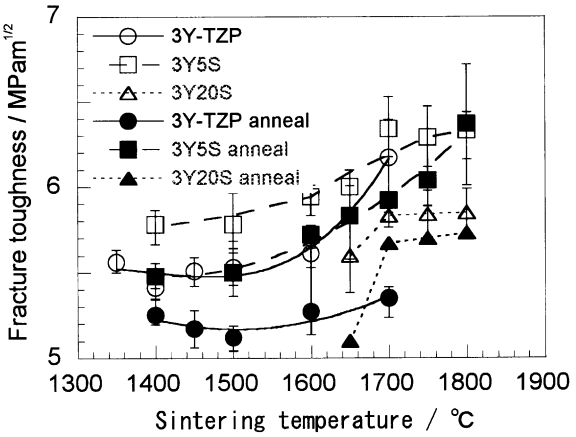


Fig. 8. The fracture toughness for 3Y-TZP monolith and 3Y-TZP/SiC nanocomposites as a function of sintering temperature. The open symbols mean the toughness before annealing and the solid ones are that after annealing at 1300 °C for 10 min in Ar.

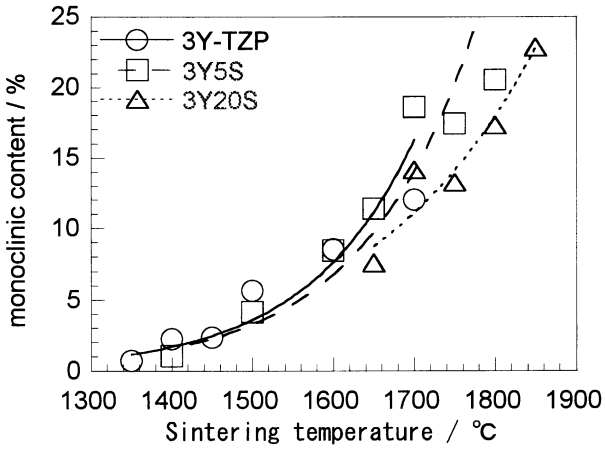


Fig. 9. The m-$ZrO_2$ content in fracture surface for 3Y-TZP monolith and 3Y-TZP/SiC nanocomposites as a function of sintering temperature.

The amount of m-$ZrO_2$ increased with increase in the sintering temperature and SiC content, which should result in improvement of fracture toughness.

## 4. Discussion

As shown in Fig. 7, the fracture strength for 3Y-TZP did not change by incorporating nano-sized SiC particles and about 1.5 GPa was achieved as maximum strength in each composition when the mixed powder was sintered at a suitable temperature. The microstructure greatly affects mechanical properties, in particular for fracture strength. The relationship between strength and defect size that relates to grain size is expressed by Griffith's equation.[30] The strength becomes higher with decreasing defect size and is also proportional to the toughness obviously. At the same sintering temperature, grain growth of 3Y-TZP matrix

was suppressed by nano-sized SiC particulate as shown in Fig. 4, however, SiC particles caused an increase in sintering temperature simultaneously to obtain the fully densified body. The toughness was improved by dispersing SiC particles as shown in Fig. 8. The maximum grain size in the 3Y-TZP monolith sintered at 1500 °C (3Y-TZP1500), 3Y5S1700 and 3Y20S at 1750 °C (3Y20S1750) which exhibited the maximum strength in each composition were 1.51, 2.48 and 1.98 μm. The maximum grain size for densified body is generally proportional to defect size. The maximum and mean grain size for fully densified composites, 3Y5S1700 and 3Y20S1750, were larger than those for 3Y-TZP1500. Since the strength depends on both defect size and fracture toughness, the large defect size should be a main reason of no improvements in strength for this 3Y-TZP/SiC nanocomposite system in spite of the improving the toughness.

The improvement of fracture toughness is taken up in this section. In common ceramics, fracture toughness is related to Young's modulus and fracture energy which is necessary to propagate a crack, and thus the increase in Young's modulus as shown in Fig. 6 should be one of the factors to improve toughness.[31] Other factors included in fracture energy term also affect toughness in this system. The fracture energy depends on some irreversible energy scatters and losses. For instance, crack deflection, bridging and/or bowing are included in irreversible energies in composite systems.[32] Furthermore, tensile residual stress in matrix induced the intragranular fracture in this nanocomposite system. The energy for intragranular facture is higher than that for intergranular fracture, improvement of fracture toughness in nanocomposites should be due to the increase in fracture energy. Additionally, compressive residual stress around SiC particles formed by the CTE mismatch led to improvement of crack bridging force. In the 3Y-TZP system, the phase transformability also influences fracture toughness, and toughness improves when transformation easily occurs. As shown in Fig. 8, fracture toughness was increased by dispersing SiC particles. However, the amount of m-$ZrO_2$ in fractural surface for composite was smaller than that for monolith at same sintering temperature as shown in Fig. 9, which means 3Y-TZP monolith was easy to transform into m-$ZrO_2$ at the same sintering temperature as nanocomposites because of large grain size. From these results, the improvement in fracture toughness for 3Y-TZP/SiC nanocomposites should be attributed to the crack deflection and residual stresses toughening mechanisms that are effective in nanocomposite systems[33] as well as phase transformation toughening. Adding SiC particles may also affect phase transformability.

Next, effect of SiC dispersoid on phase transformation which is an important toughening mechanism of 3Y-TZP is discussed. The toughness for transformation toughening materials, $K_{IC}^{t}$, can be expressed as the following equation,[34]

$$K_{IC}^{t} = K_{IC}^{m} + \frac{\eta e^{T} V_t E h^{1/2}}{1-\nu} \quad (3)$$

where $K_{IC}^{m}$, $\eta$, $e^{T}$, $V_t$, $E$, $h$ and $\nu$ are fracture toughness for matrix, a constant, strain, volume fraction of t-$ZrO_2$, Young's modulus, thickness of transformation zone and Poisson's ratio, respectively. From Eq. (3), it is obvious that the thickness of transformation zone is important factor to toughness. Transformation relates to microstructure, i.e., grain size, stabilizer content, impurity, temperature and defects.[4,35–40] Increasing stabilizer and temperature depressed the transformation,[35] meanwhile increasing defects enhances martensitic nucleation and thus the transformation is promoted.[36] The phase transformation can more easily occur with increasing grain size.[4,37–40] Fig. 10 shows fracture toughness of 3Y-TZP monolith and 3Y5S as a function of the mean grain size after annealing that eliminates the surface compressive stress layer. The 3Y5S exhibited higher toughness than the 3Y-TZP monolith even at same grain size. From Figs. 4 and 9, the m-$ZrO_2$ content in fracture surface as a function of the mean grain size is shown in Fig. 11. The m-$ZrO_2$ content increased with the grain size and SiC content, which are spontaneous phenomenon. These transformation behaviors and effects of SiC dispersion on transformation will be explained in the following parts.

First, the effect of Young's modulus on the transformation is considered. In the $ZrO_2$/SiC nanocomposite case, Young's modulus increased by adding SiC particles as shown in Fig. 6, and the composites had higher Young's modulus than monolith. According to Lange,[38] the effect of Young's modulus on the constraining matrix can be explained by assuming that the transformation

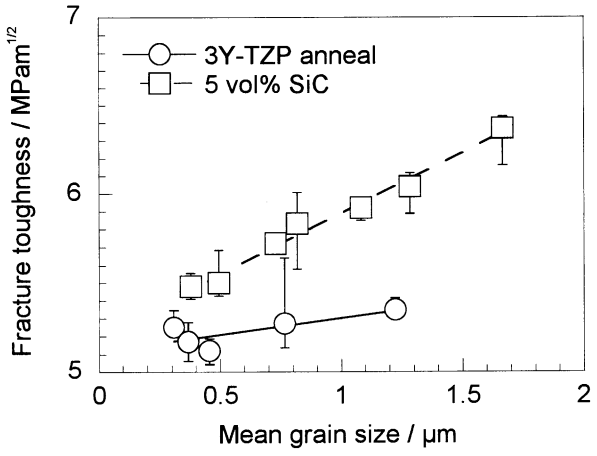


Fig. 10. The fracture toughness for 3Y-TZP monolith and 3Y-TZP/5 vol.% SiC nanocomposite after annealing at 1300 °C for 10 min in Ar as a function of the mean grain size.

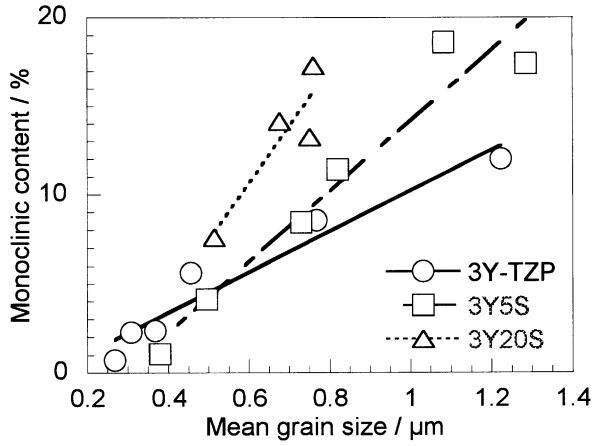


Fig. 11. The m-$ZrO_2$ content in fracture surface of 3Y-TZP monolith and 3Y-TZP/SiC nanocomposites as a function of the mean grain size.

only involves an isotropic volume expansion. Under this assumption, Eq. (4) expresses the strain energy of m-$ZrO_2$, $U_{SE}$, in the case of a spherical t-$ZrO_2$,

$$U_{SE} = \frac{1}{6}\frac{2E_1E_2}{(1+\nu_1)E_2 + 2(1-2\nu_2)E_1}\left(\frac{\Delta V}{V}\right)^2 \quad (4)$$

where $E$ and $\nu$ are Young's modulus and Poisson's ratio, and subscript 1 and 2 indicate matrix, transforming particles, $\Delta V$ and $V$ are the volume change and initial volume of transformed particles/grains, respectively. That is, the greater the Young's modulus of constraining matrix, the greater the strain energy, thus it becomes difficult to transform from t-$ZrO_2$ to m-$ZrO_2$ due to the restraint. From this theory, 3Y-TZP/SiC nanocomposites that possess higher Young's modulus than monolith oppose phase transformation. From experimental results, the increase in Young's modulus was about 10 GPa by incorporating 5 vol.% SiC particulate. Therefore t-$ZrO_2$ grains in the composites should be restrained by higher strain energy than monolith, and the transformation should be depressed. The results, however, disagreed with this theory. Then, the effects of residual stresses due to CTE mismatch between 3Y-TZP and SiC have to be taken into consideration.

Generally, the phase transformation is promoted by applied stress, and the transformation rate increases with the stress.[41] When the residual tensile stress is imposed on t-$ZrO_2$ grains, phase transformation can occur easily with aid of the stress. A t-$ZrO_2$ particle undergoes size and shape changes by the transformation from t-$ZrO_2$ to m-$ZrO_2$, which causes volume expansion about 4.6% in monolithic case.[42] Thus the material surrounding the transformed particle will oppose transformation, which is the strain energy involved in this constraint. On the other hand, the transformation can easily occur when residual tensile stress is imposed, compared with the transformation without the stress, because the stress required to transform reduces by the residual tensile stress. On the contrary, transformation may be suppressed in the case that compressive residual stress is imposed.

In the nanocomposite cases, residual stresses are accumulated in cooling process from sintering temperature due to CTE mismatch. Table 1 indicates the residual stresses calculated under the assumption that the temperatures started to accumulate the stresses are 1000 and 1400 °C.[43] Stress relaxation mechanisms by grain boundary diffusion and lattice diffusion do not work below those temperatures, and the stresses start to accumulate, respectively. The higher those temperatures, the greater the stresses become. In the case that all nano-sized particles are located within matrix grains, residual stresses become higher than the case that all particles are located at grain boundaries.[43] Under this assumption, the theoretical residual tensile stress, for example, 3Y5S, can be assumed to be between 60 and 90 MPa, because SiC particles, in fact, were located both within matrix grains and at grain boundaries as shown in Fig. 2. This tensile stress should enhance the transformation. However, this effect might be smaller than the effect of Young's modulus.

In this part, compressive stress imposed in SiC particles is taken into consideration. According to Choa,[43] when the CTE of matrix is higher than that of second phase, the formation of dislocations around dispersed particles is caused by the high compressive stress which is imposed in second phase (i.e., SiC particulate), especially for the particles within matrix grains. Generally, it is difficult to form dislocations in monolithic ceramics, but dislocations can be found easily in nanocomposites. The dislocation was observed in 3Y-TZP matrix grain as shown in Fig. 2. As mentioned before, existence of defects promotes the transformation,[36] therefore the transformation for composites easily occur comparing with the monolith due to the dislocations. The tensile stress increases and compressive stress decreases with increasing SiC content as shown in Table 1. Although compressive stress decreases with increasing SiC content, the stress may be still high enough to form dislocation. Additionally, transformation increases compressive

Table 1
Theoretical residual stresses for 3Y-TZP/SiC composite

| | Matrix/MPa | | SiC/MPa | |
|---|---|---|---|---|
| | Lattice[a] | Grain boundary[b] | Lattice[a] | Grain boundary[b] |
| 3Y5S | +90 | +60 | −1680 | −1200 |
| 3Y20S | +350 | +250 | −1410 | −1010 |

+: Tensile stress; −: compressive stress.
[a] The relaxation by lattice diffusion creep stops at 1400 °C.
[b] The relaxation by lattice and grain boundary diffusion creep stops at 1000 °C.

stress imposed on SiC particles due to volume expansion, then dislocation generated and transformation should be enhanced. Thus, the transformation is more promoted by increasing SiC content, in spite of increasing Young's modulus by SiC addition. The balance between Young's modulus and the residual stresses should determine the transformability. From the result, the effect of residual stresses is more effective than increase of Young's modulus in the 3Y-TZP/SiC nanocomposite system.

## 5. Conclusion

3Y-TZP/SiC nanocomposites were successfully fabricated by using hot pressing. The microstructure and mechanical properties of the nanocomposites were evaluated, and effects of SiC particulate on the properties of 3Y-TZP were investigated. SiC particulate inhibited densification and grain growth, and thus nanocomposites have fine and homogeneous microstructure. Nanocomposites were more easily transformed than 3Y-TZP monolith at the same grain size, because dispersed SiC particles influence the phase transformation from t-$ZrO_2$ to m-$ZrO_2$. This should be due to not only crack deflection by dispersed SiC particle with high Young's modulus, but also the phase transformation of t-$ZrO_2$ accelerated by the residual stresses from CTE mismatch between matrix and second phase. The residual stresses increase with increasing of SiC particle within matrix grain, therefore the mechanical properties of 3Y-TZP/SiC nanocomposites can be improved by dispersing smaller SiC particles.

## References


1. Masaki, T., Mechanical properties of toughened $ZrO_2$–$Y_2O_3$ ceramics. *J. Am. Ceram. Soc.*, 1986, **69**(8), 638–640.
2. Claussen, N. In *Advances in Ceramics, Science and technology of zirconia II,* Vol. 12, ed. N. Claussen, M. Rühle and A. H. Heuer. The American Ceramic Society, OH, 1984, pp. 325–351.
3. Gogotsi, G. A., Lomonova, E. E. and Pejchev, V. G., Strength and fracture toughness of zirconia crystal. *J. Eur. Ceram. Soc.*, 1993, **11**, 123–132.
4. Swain, M. V., Grain-size dependence of toughness and transformability of 2 mol% Y-TZP ceramics. *J. Mater. Sci. Lett.*, 1986, **5**, 1159–1162.
5. Gross, V. and Swain, M. V., Mechanical properties and microstructure of sintered and hot isostatically pressed yttria-partially-stabilized zirconia (Y-PSZ). *J. Aust. Ceram. Soc.*, 1986, **22**, 1–12.
6. Swain, M. V., Strength-toughness relationships for transformation toughened ceramics. In *Fracture Mechanics of Ceramics,* Vol. 7/8, ed. R. C. Bradt, A. G. Evans, D. P. H. Hasselmann and F. F. Lange. Plenum Press, New York, 1985, pp. 151–162.
7. Swain, M. V. and Rose, L. R. F., Strength limitaions of transformation-toughened zirconia alloys. *J. Am. Ceram. Soc.*, 1986, **69**(7), 511–518.
8. Sato, T., Ohtake, S. and Shimada, M., Transformation of yttria partially stabilized zirconia by low temperature annealing in air. *J. Mater. Sci.*, 1985, **20**, 1466–1470.
9. Lange, F. F., Dunlop, G. L. and Davis, B. I., Degradation during aging of transformation-toughened $ZrO_2$–$Y_2O_3$ materials at 250 °C. *J. Am. Ceram. Soc.*, 1986, **69**(3), 237–240.
10. Claussen, N., Fracture toughness of $Al_2O_3$ with an unstabilized $ZrO_2$ dispersed phase. *J. Am. Ceram. Soc.*, 1976, **59**, 49–51.
11. Dougherty, S. E., G Nieh, T., Wadsworth, J. and Akimune, Y., Mechanical properties of a 20 vol% SiC whisker-reinforced, yttria-stabilized, tetragonal zirconia composite at elevated temperatures. *J. Mater. Res.*, 1995, **10**(1), 113–118.
12. Claussen, N., Weisskopf, K.-L. and Rühle, M., Tetragonal zirconia polycrystals reinforced with SiC whiskers. *J. Am. Ceram. Soc.*, 1986, **69**(3), 288–292.
13. Hong, J., Gao, L., Shaw, B. A. and Thompson, D. P., SiC platelet and SiC platelet-alumina reinforced TZP matrix composites. *Br. Ceram. Trans.*, 1995, **94**(5), 201–204.
14. Miao, X., Rainforth, W. M. and Lee, W. E., Dense zirconia-SiC platelet composites made by pressureless sintering and hot pressing. *J. Eur. Ceram. Soc.*, 1997, **17**, 913–920.
15. Lee, H. L. and Lee, H. M., Effect of SiC on the mechanical properties of 3Y-TZP/SiC composites. *J. Mater. Sci. Lett.*, 1994, **13**, 974–976.
16. Niihara, K., New design concept of structural ceramics-ceramic nanocomposites. *J. Ceram. Soc. Jpn.*, 1991, **99**(10), 974–982.
17. Hirano, T., Izaki, K. and Niihara, K., Microstructure and thermal conductivity of $Si_3N_4$/SiC nanocomposites fabricated from amorphous Si–C–N precursor powders. *Nanostruct. Mater.*, 1995, **5**(7–8), 809–818.
18. Niihara, K., Nakahira, A., Uchiyama, T. and Hirano, T., High-temperature mechanical properties of $Al_2O_3$–SiC composites. In *Fracture Mechanics of Ceramics,* Vol. 7, ed. R. C. Bradt, A. G. Evans, D. P. H. Hasselmann and F. F. Lange. Plenum Press, New York, 1986, pp. 103–116.
19. Ohji, T., Nakahira, A., Hirano, T. and Niihara, K., Tensile creep behavior of alumina/silicon carbide nanocomposite. *J. Am. Ceram. Soc.*, 1994, **77**(12), 3259–3262.
20. Ohji, T., Hirano, T., Nakahira, A. and Niihara, K., Particle/matrix interface and its role in creep inhibition in alumina/silicon carbide nanocomposites. *J. Am. Ceram. Soc.*, 1996, **79**(1), 33–45.
21. Sternitzke, M., Structural ceramic nanocomposites. *J. Eur. Ceram. Soc.*, 1997, **17**, 1061–1082.
22. Sasaki, G., Nakase, H., Suganuma, K., Fujita, T. and Niihara, K., Mechanical properties and microstructure of $Si_3N_4$ matrix composite with nano-meter scale SiC particles. *J. Ceram. Soc. Jpn.*, 1992, **100**(4), 536–540.
23. Yasuda, E., Bao, Q. and Niihara, K., The effects of fine SiC particles on the creep of MgO at high temperature. *J. Ceram. Soc. Jpn.*, 1992, **100**(4), 514–519.
24. Niihara, K., Morena, R. and Hasselman, D. P. H., Evaluation of $K_{1c}$ of brittle solids by the indentation method with low crack-to-indent ratios. *J. Mater. Sci. Lett.*, 1982, **1**(1), 13–16.
25. Toraya, H., Yoshimura, M. and Somiya, S., Calibration curve for quantitative analysis of the monoclinic-tetragonal $ZrO_2$ system by X-ray diffraction. *J. Am. Ceram. Soc.*, 1984, **6**, C–119.
26. Ding, Z., Oberacker, R., Frei, H. and Thümmler, F., Consolidation of Y-TZP/SiC particulate composites by sintering and containerless post-HIPing. *J. Eur. Ceram. Soc.*, 1992, **10**, 255–261.
27. Taya, M., Hayashi, S., Kobayashi, A. S. and Yoon, H. S., Toughening of a particulate-reinforced ceramic-matrix composites by thermal residual stress. *J. Am. Ceram. Soc.*, 1990, **73**(5), 1382–1391.
28. Kagawa, Y. and Hatta, H., *Tailoring Ceramic Composites*. Agune Shouhusha, Tokyo, 1990 (in Japanese).
29. Claussen, N. and Rühle, M., Design of transformation-toughened ceramics. In *Advances in Ceramics, Vol. 3, Science and Technology of Zirconia,* ed. A. H. Heuer and L. W. Hobbs. Am. Ceram. Soc. 1982, pp. 137–163.
30. Kingery, W. D., Bowen, H. K. and Uhlmann, D. R., *Introduction to Ceramics*, 2nd ed.. John Wiley & Sons, New York, 1976.

31. Nishida, T., In *Mechanical Properties Evaluation for Ceramics*, edn. T. Nishida and E. Yasuda. Nikkan Kogyo Press, Tokyo, 1986, p. 100 (in Japanese).
32. Kagawa, Y. and Htta, H., *Tailoring Ceramic Composites*. Agune Shouhusha, Tokyo, 1990, pp. 120–126 (in Japanese).
33. Ohji, T. and Niihara, K., Comments on "physical limitations of the inherent toughness and strength in ceramic-ceramic and ceramic-metal nanocomposites". *J. Ceram. Soc. Jpn*., 1996, **104**(6), 581–582.
34. McMeeking, R. M. and Evans, A. G., Mechanics of transformation-toughening in brittle materials. *J. Am. Ceram. Soc*., 1982, **65**(5), 242–246.
35. Yoshimura, M., Phase stability of Zirconia. *Ceram. Bull*., 1988, **67**(12), 1950–1955.
36. Chen, I. W., Chiao, Y. H. and Tsuzaki, K., Statistics of martensitic nucleation. *Acta Metall*., 1985, **33**(10), 1847–1859.
37. Lange, F. F. and Green, D. J., Effect of inclusion size on the retention of tetragonal $ZrO_2$: theory and experiments. In *Advances in Ceramics, Vol. 3, Science and Technology of Zirconia,* ed. A. H. Heuer and L. W. Hobbs. Am. Ceram. Soc., OH, 1981, pp. 217–225.
38. Lange, F. F., Transformation toughening Part 1. Size effects associated with the thermodynamics of constrained transformations. *J. Mater. Sci*., 1982, **17**, 225–234.
39. Müller, I. and Müller, W., Size effect on transformation temperature of zirconia powders and inclusions. In *Advances in Ceramics, Vol. 12, Science and Technology of Zirconia II,* ed. N. Claussen, M. Rühle and A. H. Heuer. Am. Ceram. Soc., OH, 1984, pp. 443–454.
40. Garvie, R. C. and Swain, M. V., Thermodynamics of the tetragonal to monoclinic phase transformation in constrained zirconia microcrystals Part 1. In the absence of an applied stress field. *J. Mater. Sci*., 1985, **20**, 1193–1200.
41. Matsui, M., Soma, T. and Oda, I., Stress-induced transformation and plastic deformation for $Y_2O_3$-containing tetragonal zirconia polycrystals. *J. Am. Ceram. Soc*., 1986, **69**(3), 198–202.
42. Yanagida, H. *et al*., *Cyclopedia of Fine Ceramics*. Gihodo Press, Tokyo, 1987 (in Japanese).
43. Choa, Y. H., *Strengthening and Toughening Mechanisms for MgO/SiC and Related Nanocomposites*. PhD thesis, Osaka University, Osaka, 1996.